EXPERIMENTAL INVESTIGATION ON THE EFFECT OF COPPER UPON EUTECTOID TRANSFORMATION OF AS-CAST AND AUSTENITIZED SPHEROIDAL GRAPHITE CAST IRON

J. Sertucha and P. Larrañaga
AZTERLAN, Durango (Bizkaia) Spain

J. Lacaze
Université de Toulouse, CIRIMAT, Toulouse, France

M. Insausti
Universidad del País Vasco, Bilbao (Bizkaia), Spain

Abstract

Copper is known as a pearlite promoter in cast iron and has been used as such for a long time, most often together with low amounts of manganese. Literature data, however, has shown that these two elements act differently on the ferritic and pearlitic transformations. In order to provide more insight in the role of this element on the solid-state transformation of spheroidal graphite (SG) cast iron, this paper investigates the effect of adding copper in small step increments, from 0.11 to 1 wt. % Cu, to SG irons containing about 0.15 wt. % Mn.

The characteristic temperatures for the stable and metastable eutectoid transformations as recorded during cooling after solidification in standard cups and after austenitizing are presented together with microstructure information. It is found that a copper content of about 0.6 wt. % is the upper limit over which only small amounts of ferrite could be obtained except at very low cooling rates. This is tentatively related to the lowering of the temperature for ferrite and the associated decreased kinetics for austenite decomposition in the stable system.

Keywords: *pearlite, eutectoid, metastable, ferrite, transformation temperature*

Introduction

The use of selective additions for promoting pearlite formation in cast irons has become common practice a long time ago, with emphasis on low-cost elements such as copper, manganese, arsenic and tin.[1] Conversely, the presence of such species in foundry returns and scraps may lead to difficulties in achieving fully ferritic matrices. The need for appropriate control of melt composition before casting has thus triggered extensive experimental studies.[1,2] While tin and arsenic become effective at very low levels, they are associated with environmental hazards so that metallic elements such as manganese and copper are preferred.

The way copper and manganese act on the eutectoid transformation has lead to several, potentially contradictory, explanations as reviewed by Pan et al.[2] It was claimed in a more recent study that the major effect of metallic alloying additions is to change the relative position of the stable and metastable eutectoid transformation temperature ranges.[3] More precisely, it has been suggested that ferrite and pearlite do inherit the composition of the parent austenite in substitutional elements because there is not time enough for their long range redistribution.[4,5] Accordingly, the temperature at which the transformation may start upon cooling at a finite rate was shown to be the lowest temperature of the three-phase field in the isopleth sections corresponding to the alloy composition[5,6], as shown in Figure 1. This reference temperature will be denoted as T_α for the stable transformation and T_p for the metastable one. These temperatures could be calculated by means of a thermodynamic software and appropriate databank and expressed as:

$$T_\alpha(°C)=739+18.4w_{Si}+2.0(w_{Si})^2-14.0w_{Cu}-45.0w_{Mn} \quad \text{Equation 1}$$

$$T_p(°C)=727+21.6w_{Si}+0.023(w_{Si})^2-21.0w_{Cu}-25.0w_{Mn} \quad \text{Equation 2}$$

with eventually additional terms for Mo, Cr, Ni.[7] This analysis has been verified with some success to literature data[7] concerning the temperature for the start of the stable and metastable transformations. Also, it could be demonstrated using literature data[1,2] that the growth rate of pearlite is not significantly affected by additions of Cu, Mn, As or Sn at the levels generally used.[8]

Further, it has been shown that low level addition of copper to a Mn-free cast iron does not promote pearlite[3,5] and this may be understood by observing that copper decreases T_α much less than T_p. The effect of manganese is just the opposite, hence its strong pearlite promoter effect. Accordingly,

it was found that small amounts of Cu can counteract the effect of low level addition of manganese.[3] On the contrary, the addition of 1 wt. % of copper definitely had a pearlite promoter effect. The present series of experiments was intended at providing further experimental data for small increments in copper contents from 0.11 up to 1 wt. % so as to lead to a clearer understanding of its effect on the eutectoid transformation. For that purpose, use has been made of thermal analysis during cooling of nodular cast irons with various amounts of Cu, either straight after solidification or after an austenitizing treatment.

Experimental

Melts were prepared in medium frequency induction furnaces of 6 and 10 t capacity using metallic charges made from 25% of pig iron, 25% of automotive steel scrap and 50% of classified returns. After melting, carbon and silicon contents were corrected as a function of thermal analysis tests performed using the Thermolan® system[9] and of spectrometry analysis on a metal sample for other chemical elements. Additions of C and Si to the melt were performed using electrode graphite and FeSi 75% master alloy, respectively. At the same time, SiC was added into the induction furnace to increase the nucleation potential of the melt. The temperature of the melt was then increased to 1490-1500ºC (2714-2732°F) after the corrections have been made, and its surface was skimmed. The spheroidization treatment was achieved with a magnesium alloy (46.7% Si, 5.2% Mg, 2.2% Ca, 1.8% Re and 1.1% Al, in wt. %) at about 1440-1470ºC (2624-2678°F) using the tundish-cover method into a ladle of 2 t capacity. The change in Cu content was realized by adding various amounts of Cu (99.9% of purity) together with the steel cover for magnesium treatment. After the reaction was completed, the slag was removed from the melt surface and the batch was transferred to a pouring furnace. To check the chemical composition of the treated melts, metal samples were taken just before picking up the iron from the pouring furnace and were analysed by combustion techniques using Leco CS 244 equipment for determining C and S contents, gravimetric procedures for Si and optical emission spectrometry (OBLF QS750) for other elements. From the melts cast, one ferritic grade (NF3) and seven pearlitic grades (NP1 to NP7) obtained by adding different amounts of Cu will be considered in the present work. The compositions of the alloys are listed in Table 1 where the expected accuracy for each element is indicated.

The liquid-solid and solid-solid transformations of as-cast materials were investigated by means of standard thermal analysis (TA) cups with geometric modulus 0.62-0.63 cm. Before pouring the cups, 0.20% (of the weight of the sample) of a commercial inoculant (0.2-0.5 mm in size with chemical composition given as: 70-78% Si, 3.2–4.5% Al, 0.3–1.5% Ca, 0.5% Re, in wt. %) was added into the cups. The cooling curves were recorded in the range of 1210-600ºC (2210-1112°F) and were analysed using the Thermolan® system.[9]

For studying solid state transformation after austenitization, cylindrical samples of 30 and 17 mm in diameter and 30 and 20 mm in length were machined out from the TA cups. These samples were then introduced in a temperature-controlled tubular furnace in which they were first heated for holding at a temperature in the range 850 to 1000°C (1562 to 1832°F) and then cooled. Four different cooling rates (V_{cool}) were achieved by switching off the power and varying the position of the sample along the axis of the furnace. These four cooling conditions will be labelled U1 to U4. The temperature versus time evolution of the material was recorded using K-type thermocouples located in the centre of the samples. Finally, cylinders of 3-4 mm in diameter and 2 mm in length were obtained from the as-cast cups and analysed using a TA SDT 2960 instrument. In these experiments, aluminium oxide was used to fill the reference holder. The samples were heated to 950ºC (1742°F), held at that temperature for 20 min, and then cooled down to room temperature. Three cooling rates were used, 5, 10 and about 38 K/min, the latter being obtained as the maximum achievable cooling rate of the DTA-TGA apparatus.

The evaluation of the experimental nodule counts (denoted as N) and the characterisation of solid-state structures were carried out through metallographic analysis by means of optical microscopy made on as-cast and austenitized samples. Nodule counts and ferrite contents were evaluated on different micrographs obtained at a magnification of ×100 in the central area of the samples using Leica image analysis software. For each sample, measurements were performed on three different fields.

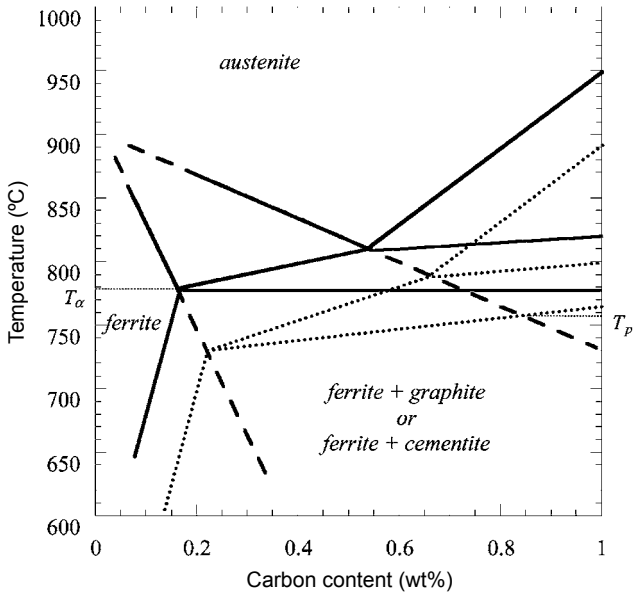

Figure 1. Schematic isopleths section of the Fe-C-Si phase diagram in the temperature range of the eutectoid reaction. Solid lines correspond to the stable system ferrite/austenite/graphite and dotted lines are related to the metastable system ferrite/austenite/cementite.

Results

The cooling curves obtained from the TA cups all showed similar results for the solidification step in terms of minimum temperature and recalescence during the eutectic solidification. The measured nodule counts, N, are in the range 250-280 mm^{-2}, and listed in Table 2. This similarity in the nodule count of the various cast metals gives adequate conditions for comparing the characteristics of the solid-solid transformation. As an example, Figure 2-a shows the cooling curve recorded from the TA cup cast with alloy NP6, as well as the time derivative of this curve. From the latter, it is seen that the solid state transformation relates to a clear peak that starts at a temperature significantly higher than the plateau observed on the cooling curve. Because the microstructure of all TA cups showed some ferrite to be present (see Table 2), it was assumed that the start temperature relates to the formation of this phase and was accordingly denoted as $T_{\alpha,exp}$.

Table 1. Alloy Chemical Composition (wt. %)*

Alloy	C (0.06)	Si (0.02)	Mn (0.01)	P (0.004)	S (0.001)	Cu (0.005)	Mg (0.004)	Cr (0.002)	T	T_p	$T - T_p$
NF3	3.79	2.51	0.19	0.029	0.001	0.11	0.032	0.02	790.8	777.3	13.5
NP1	3.76	2.47	0.19	0.032	0.002	0.18	0.037	0.02	788.6	774.9	13.7
NP2	3.62	2.65	0.16	0.030	0.003	0.32	0.033	0.02	793.5	776.8	16.7
NP3	3.68	2.69	0.12	0.028	0.003	0.44	0.027	0.02	794.9	776.2	18.7
NP4	3.63	2.83	0.13	0.031	0.002	0.55	0.036	0.02	797.3	776.9	20.4
NP5	3.62	2.74	0.14	0.031	0.004	0.66	0.034	0.03	792.2	772.4	19.8
NP6	3.74	2.51	0.18	0.033	0.002	0.68	0.035	0.03	783.0	765.7	17.3
NP7	3.64	2.51	0.14	0.034	0.004	0.95	0.033	0.02	781.3	760.9	20.4

Note: * Numbers between brackets give the accuracy for each element. T_α and T_p are the calculated lower bounds of the three phase fields in the stable and metastable systems, respectively.

Table 2. Characteristics of the Cooling Curves and Metallographic Results from TA Cups

Alloy	V_{cool} (K/min)	$T_{\alpha,exp}$	$T_{p,exp}$	T_{trans} (ºC)	V_{trans} (K/s)	N (mm^{-2})	Ferrite fraction (%)
NF3	60.0	770	-	742.3	-0.10	271	75
NP1	60.1	747	-	734.7	-0.13	262	65
NP2	64.3	760	-	734.2	-0.14	262	65
NP3	60.9	776	-	730.5	-0.11	250	60
NP4	59.5	773	-	726.8	-0.06	287	60
NP5	57.5	755	723	723.5	0.00	275	35
NP6	61.0	734	713	715.0	0.13	274	20
NP7	59.6	743	712	714.1	0.12	258	10

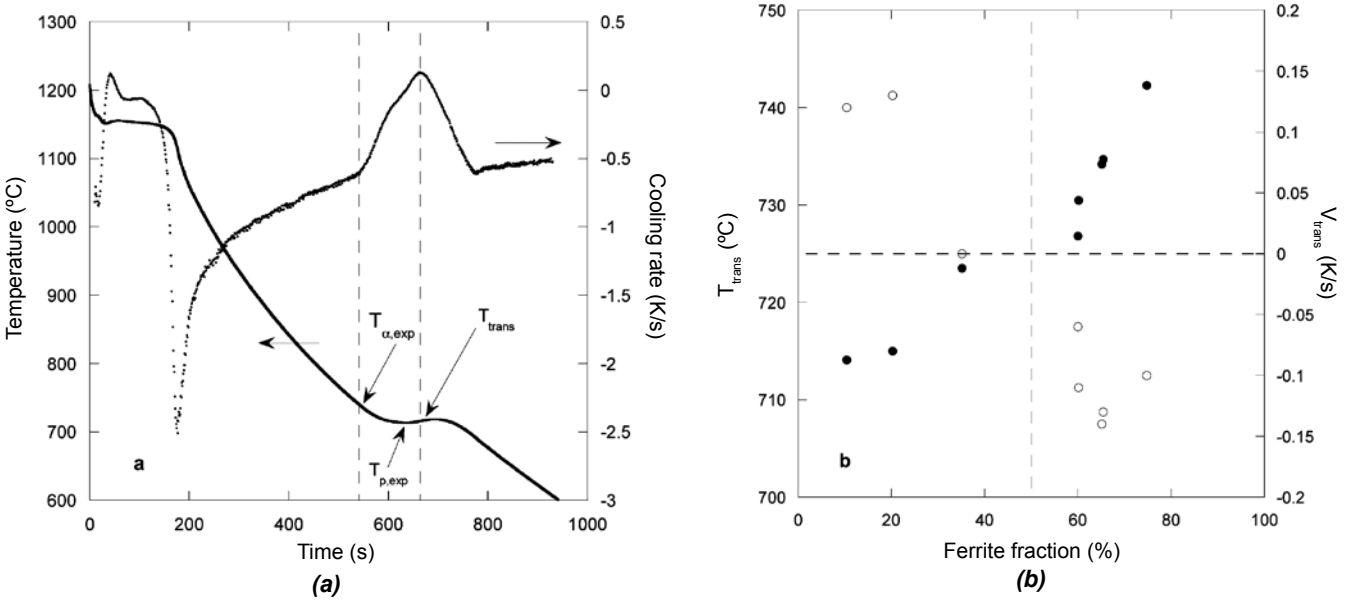

Figure 2. (a) Cooling curve and its time derivative obtained from the TA-cup cast with NP6; (b) relation between the final fraction of ferrite and the characteristics of the eutectoid transformation, V_{trans} (open circles) and T_{trans} (solid circles).

Conversely, all TA cup materials contained some pearlite (see Table 2) though only the cooling curve of the three alloys with highest Cu content showed a clear recalescence or a marked arrest that could be associated with pearlite formation. The minimum temperature recorded in such cases has been labelled $T_{p,exp}$ in Figure 2-a. Because the formation of pearlite was not always evident, the cooling curves were also characterized with the maximum rate of temperature change during the eutectoid transformation, V_{trans}, and the corresponding temperature, T_{trans}. Finally, for comparison purposes with other experiments, the cooling rate was evaluated by means of its average value V_{cool} within the range 920-775ºC (1688-1427 °F) again given in Table 2.

Table 3. Cooling Curves Characteristics Obtained from the U1-U4 Furnace Experiments*

		NF3	NP1	NP2	NP3	NP4	NP5	NP6	NP7
U1	V_{cool} (K/min)	4.7	4.6	4.7	4.8	4.7	4.8	4.4	4.4
	$T_{\alpha,exp}/T_{p,exp}$ (ºC)	783/-	783/-	782/-	782/-	783/-	774/736	771/731	-/726
	V_{trans} (K/s)	-0.13	-0.12	-0.15	-0.12	-0.12	0.01	0.03	0.02
	T_{trans} (ºC)	773	769	767	758	752	737	735	730
	Ferrite (%)	100	98	98	90	100	62	60	41
U2	V_{cool} (K/min)	10.1	9.4	10.0	9.9	10.3	9.2	9.8	9.8
	$T_{\alpha,exp}/T_{p,exp}$ (ºC)	782/-	778/-	772/-	751/-	771/-	760/731	-/714	-/723
	V_{trans} (K/s)	-0.07	-0.13	-0.13	-0.14	-0.14	0.01	0.09	0.04
	T_{trans} (ºC)	758	755	756	723	742	732	716	726
	Ferrite (%)	98	98	82	73	79	59	20	21
U3	V_{cool} (K/min)	44.1	55.7	33.9	66.4	45.3	55.5	35.0	65.1
	$T_{\alpha,exp}/T_{p,exp}$ (ºC)	746/-	751/-	754/-	743/-	753/-	718/711	-/716	-/706
	V_{trans} (K/s)	-0.04	-0.13	-0.08	-0.04	-0.07	0.05	0.03	0.15
	T_{trans} (ºC)	727	722	731	721	724	711	717	706
	Ferrite (%)	82	98	95	95	98	35	22	5
U4	V_{cool} (K/min)	197.9	190.9	202.8	159.1	183.8	186.8	146.9	143.7
	$T_{\alpha,exp}/T_{p,exp}$ (ºC))	719/707	711/696	722/695	703/689	699/692	697/689	-/692	694
	V_{trans} (K/s)	0.21	0.1	0.11	0.09	0.11	0.18	0.46	0.32
	T_{trans} (ºC)	710	696	696	690	692	688	697	694
	Ferrite (%)	46	45	35	43	51	42	2	5

Note: *Reference cooling rate V_{cool} (K/min), $T_{\alpha,exp}$ (°C), $T_{p,exp}$ (°C), V_{trans} (K/s) and T_{trans} (°C). The ferrite fraction (%) is also listed.

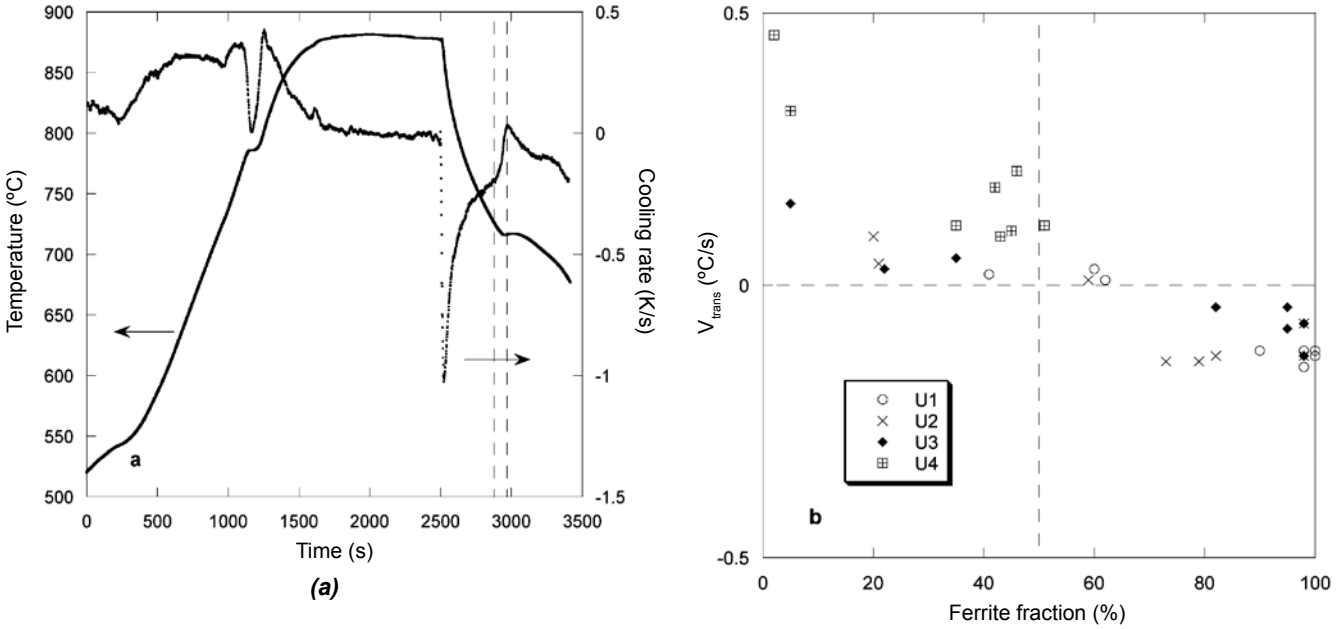

Figure 3. (a) Temperature-time evolution during heat treatment in the furnace and its derivative during trial U3 on alloy NP6; (b) relationship between ferrite fraction and V_{trans} for the whole series of U samples.

Figure 2-b shows that increase in ferrite content is associated with higher values of T_{trans} (solid circles) and more negative values of V_{trans} (open circles). This is in agreement with the usual view that the ferritic transformation starts before (i.e. at higher temperature) than the pearlitic one upon cooling.

Figure 3-a illustrates the temperature evolution and its time derivative recorded during one of the heat treatments performed in the tubular furnace, including the heating and cooling stages. It is seen that the cooling stage shows features similar to those of the records obtained from the TA cups, so that the same characteristics as before could be determined. The results are listed in Table 3 where the measured ferrite fractions are also given. In Figure 3-b the ferrite fractions versus V_{trans} are plotted for this series of experiments, where the various symbols used differentiate the cooling conditions (U1 to U4) but not the alloys. It is seen that the evolution is similar to the one observed in Figure 2-b for as-cast alloys, and the same similarity was also noted with T_{trans}.

Finally, Figure 4 shows an example of a DTA record obtained upon cooling for alloy NF3. On most of the DTA records, two peaks could be identified that have been associated to the formation of ferrite for the one at higher temperature and of pearlite for the second one. The associated $T_{\alpha,exp}$ and $T_{p,exp}$ temperatures were generally estimated at the intersection of the base line and signal extrapolations as illustrated for $T_{\alpha,exp}$ in Figure 4. When pearlite growth showed up as a small peak on the DTA curve, the associated temperature $T_{p,exp}$ was better characterized by the temperature corresponding to the local minimum in the DTA signal (Figure 4). The transformation temperatures thus obtained are listed in Table 4.

Discussion

Figure 5-a illustrates, in the case of alloy NP1, the marked lowering of the phase transformation temperatures when the cooling rate is increased. It is seen that the pearlitic transformation starts at a temperature much lower than the ferritic one at a low cooling rate. The difference decreases with increasing cooling rate. Also, it may be noted that the T_{trans} temperature shifts from $T_{\alpha,exp}$ to $T_{p,exp}$ when the cooling rate is increased, and thus characterizes the whole process of austenite decomposition rather than one of the two eutectoid transformations.

To account for the composition difference between the alloys, it seems more appropriate to look at the effect of the cooling rate on the undercooling (T_{ref}-T_{exp}), where T_{ref} and T_{exp} are the reference and experimental temperatures for either the ferritic (α) or pearlitic (p) transformations. The reference temperatures have been calculated using the relationships given by equations 1 and 2, considering the content of the matrix in each substitutional solute to be 1.05 times the nominal content of the alloy in order to account for the presence of graphite. They are listed in Table 1. It is seen that the reference temperatures for the ferritic and pearlitic transformations change by more than 15°C (59°F) because of the composition changes.

The evolution of T_{ref}-T_{exp} (undercooling) is shown in Figure 5-b where open symbols (and crosses for NF3) are for the ferritic reaction and solid symbols (and plus signs for NF3) are for the pearlitic one. As expected, it is seen that the undercooling of both the ferritic and pearlitic transformations increases with cooling rate. Moreover, in line with previous works, it seems that the undercooling values for the ferritic transformation could extrapolate to zero at zero cooling rate, while a minimum undercooling of 30 to 50°C (86 to 122°F) appears necessary for the pearlitic reaction to start. It is also seen in the figure that the rate of increase of the undercooling with cooling rate is higher for the ferritic reaction than for the pearlitic one. Thus, the two series of points cross each other for a cooling rate of about 150-200 K/min, beyond which virtually no ferrite would appear. These features have been emphasized in Figure 5b with the interrupted line drawn through each of the two series of points.

It is also noted that the data in Figure 5-b appears quite scattered and this could not be related to the copper content of the alloys, neither for the ferritic reaction nor for the pearlitic one. Indeed, an effect of the copper content on the under-

Table 4. Characteristic Temperatures ($T_{\alpha,exp}$/$T_{p,exp}$) Obtained from the DTA Records

Alloy	V_{cool} (K/min)		
	5	10	38
NF3	783/749	779/725	764/716
NP1	778/728	773/722	757/710
NP2	780/?	776/719	757/711
NP3	794/725	772/719	763/707
NP4	789/731	781/733	762/713
NP5	784/731	781/723	763/719
NP6	763/727	755/718	-/713
NP7	749/723	-/718	-/707

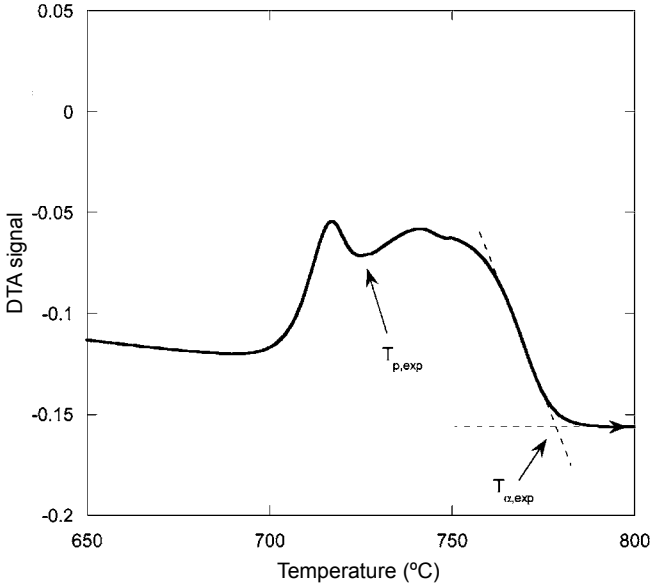

Figure 4. Example of DTA record (alloy NF3, cooling rate of 10 K/min).

cooling of the pearlitic reaction was not expected as it has been shown that limited additions of Cu, Mn, As or Sn do not affect growth kinetics of pearlite in cast irons.[8] The lack of correlation between copper content and undercooling for the start of the ferritic reaction lead to Figure 6 where the amount of ferrite is plotted as a function of the Cu content for the various cooling conditions available, i.e. for the U series as well as for the as-cast samples. The effect of Cu on the eutectoid reaction is evident. It clearly appears that 0.6 wt. % Cu is a critical limit for cast irons with 0.1 to 0.2 wt. % Mn. Above this limit a significant amount of ferrite could precipitate only at low cooling rates. For low levels of Cu, from 0.1 to 0.6 wt. %, the amount of ferrite decreases slowly for the as-cast material, while it remains nearly constant for U materials (with the possible exception of the U2 series).

This evolution of the final ferrite fraction with Cu in the range 0 to 0.6 wt. % could appear in line with the previous result that a low level of Cu counteracts the effect of manganese.[3] A possible reason of this effect could be that Cu opens the window (T_α-T_p) for the ferritic reaction, i.e. that contrary to manganese it decreases T_α less than T_p (see equations 1 and 2). However, it is seen in Table 1 that the Cu addition was associated with an increase of the Si content in the present series of castings. Thus, both the temperature T_α and the window (T_α-T_p) did increase when the Cu content varied from 0.11 to 0.6 wt. Thus, it is quite possible that the effect observed in Figure 6 is also due to an increase of the start temperature for the ferritic reaction. This effect of the transformation temperature appears evident when noting that T_α decreases strongly from alloys NP4 to NP7, i.e. for Cu contents from 0.55 to 0.95 wt. %, while the window (T_α-T_p) remains at about the same value for these four alloys.

The drastic decrease of the ferrite fraction above 0.6 wt.% Cu suggests that copper does not only affect the start temperature and the window for the ferritic reaction as postulated previously[3], but should also change the growth kinetics of ferrite. In order to verify this effect, the DTA records of the whole series of alloys were compared for the three cooling rates available. The records on alloys NF3 (ferritic) and NP6 (pearlitic) for a cooling rate of 5 K/min are plotted in Figure 7. On both curves, the arrests at highest and lowest temperatures relate respectively to the ferritic and pearlitic transformations, as already mentioned in relation with Figure 4. The intermediate bump on the record of alloy NF3 (open arrow) is due to the Curie transformation of ferrite. The comparison of these two records shows that the growth rate of ferrite is much smaller in the case of alloy NP6 than for alloy NF3. As a matter of fact, a continuous decrease of the ferrite growth rate was observed with increased addition of copper from alloy NF3 to alloy NP7 for all three cooling rates investigated with DTA. Such an effect appears far too marked to be due only to the slight temperature difference for the start of the ferritic reaction that is observed. It is here postulated that the effect is mainly due to the sharp decrease of the carbon diffusion coefficient in ferrite at the Curie temperature as assessed by Ågren.[10] Though the Curie temperature could not always be observed on the DTA traces, it is estimated at 744°C (for alloy NF3 from Figure 7 and should be similar for all other alloys as they contain about the same

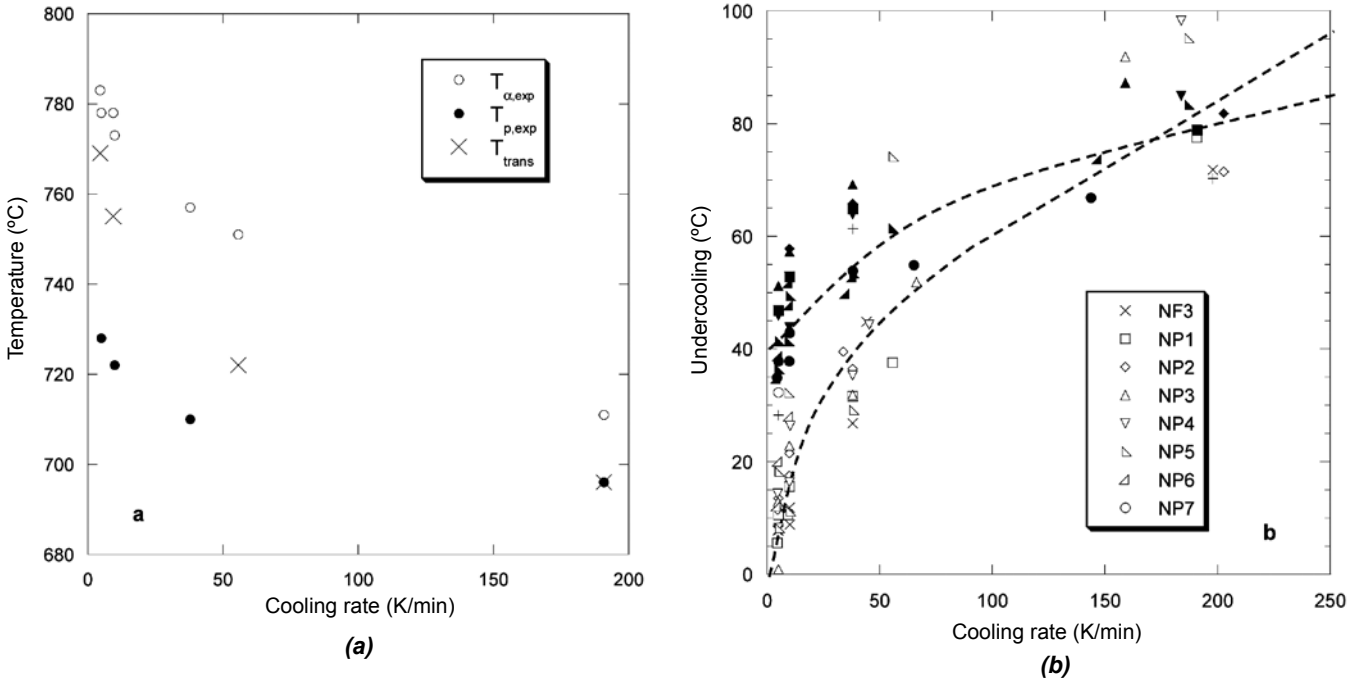

Figure 5. (a) Evolution of the characteristic transformation temperatures with the cooling rate for alloy NP1; (b) evolution of the undercooling of the ferritic (open symbols and crosses) and pearlitic (solid symbols and plus signs) reactions for all alloys and cooling rates.

silicon content than NF3. The time derivative of the DTA signal showed that the ratio of the maximum growth rate of ferrite for alloy NF3 and NP6 to be 18.9/3.6=5.25. This value compares well with the 3.7 value estimated by Ågren[10] as the jump of the carbon diffusion coefficient at the Curie temperature, thus supporting the present hypothesis.

Figure 6 also shows that at a cooling rate of about 60 K/min, as-cast (TA cups) and heat-treated (U3) materials do present very different ferrite contents. This positive effect of heat-treating on the ferrite fraction has been already reported[5] and was tentatively related to the recrystallization of the matrix upon re-austenitizing, resulting in higher number of rapid diffusion paths for carbon from austenite to graphite. Further, it was noted that high Cu addition leads to the formation of intergranular ferrite[3], and this was observed again in the present study as illustrated in Figure 8. In this figure are shown the microstructures of alloys NF3 and NP5 from samples cooled at two different rates selected so that they show a similar final amount of ferrite. It is clearly seen in Figure 8-b that part of the ferrite is intergranular, while there is no such feature in Figure 8-a.

The effect of heat-treating may also be illustrated by plotting T_{trans} and V_{trans} as a function of ferrite fraction for the as-cast and U3 samples (Figures 9-a and -b). At low ferrite fraction, it is seen that the pearlitic reaction proceeds at about the same temperature for as-cast and heat-treated alloys, but with a higher transformation rate (higher V_{trans} values) for the former. On the right side of the graphs, when the transformation is essentially ferritic, it is seen that the transformation temperature is lower and the rate of transformation higher for heat-treated samples than for as-cast ones. It is not expected that the austenitizing treatment could

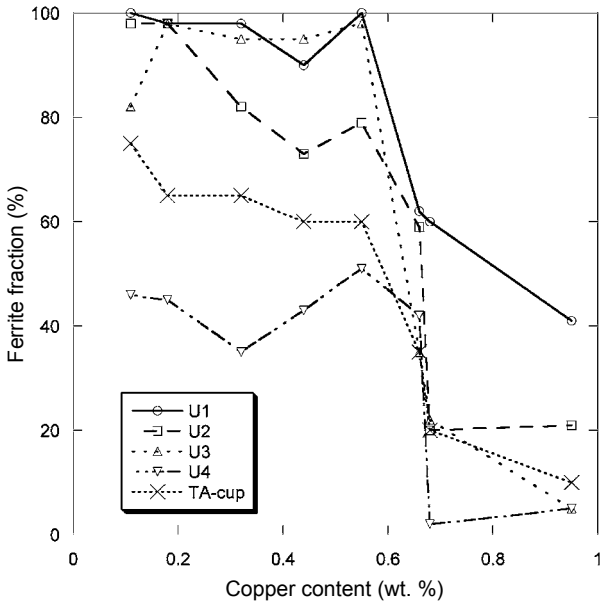

Figure 6. Evolution of the ferrite fraction with copper content for various cooling conditions.

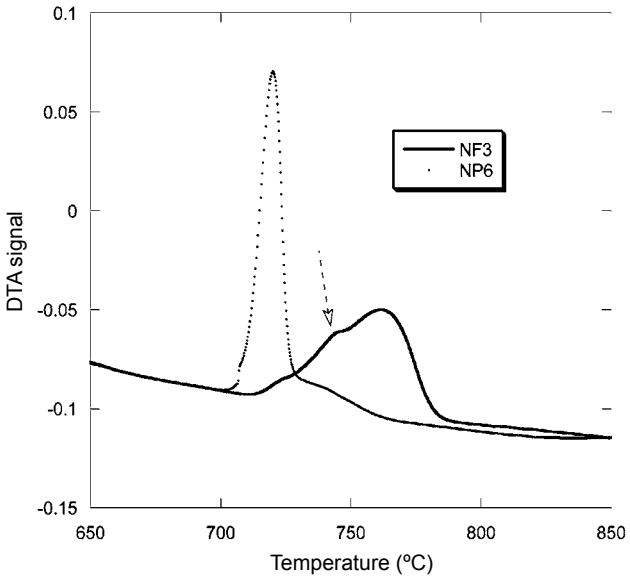

Figure 7. Comparison of the DTA traces recorded on alloys NF3 and NP6 at 5 K/min. The open arrow indicates the Curie transformation of the ferrite matrix in alloy NF3.

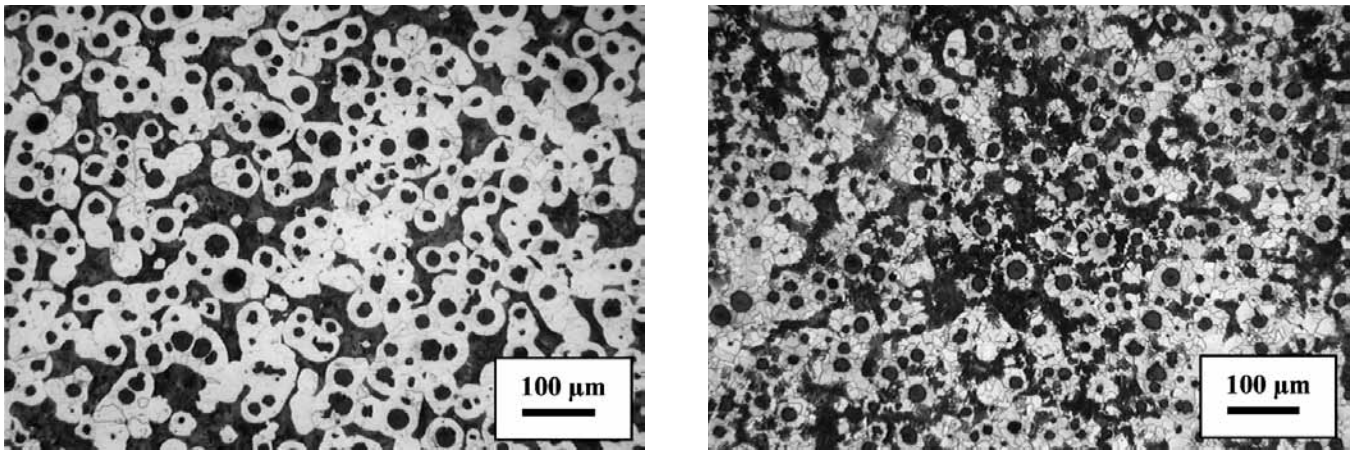

(a) ***(b)***

Figure 8. Comparison of the microstructure of alloys NF3 and NP5 after cooling at, respectively, 5 K/min and 55.5 K/min (Nital etchant).

affect significantly the microsegregation of substitutional elements, while it can certainly homogenize carbon distribution. A full understanding of the above features would thus certainly need a simulation of the microstructure evolution during the eutectoid transformation accounting for carbon redistribution. Note that the maximum ferrite content in as-cast condition is 80% whereas nearly fully ferritic structures are obtained after heat treatment.

Conclusion

A series of cast irons with copper content varying from 0.11 to 0.95 wt. % have been cast and then austenitized and cooled at different rates. The observation of their microstructure confirmed that low level addition of copper to cast irons containing 0.1-0.2 wt. % of manganese does not decrease the final ferrite amount significantly under both as-cast and heat-treated conditions. On the contrary, addition of copper at a level equal or higher than 0.6 wt. % leads to a marked decrease of the ferrite fraction at all cooling rates. Analyzing the thermal records confirmed previous results that copper addition decreases the temperature for the start of both the ferritic and pearlitic reactions, but this could not explain the dramatic change beyond 0.6 wt. % Cu added. Comparing the DTA records showed this decrease to be due to an effect of copper on the growth kinetics of ferrite which is tentatively related to the strong decrease of the carbon diffusion coefficient in ferrite when the temperature drops below the Curie temperature of that phase.

Acknowledgments

This work has been supported by the Diputación Foral de Bizkaia and the Science and Technology Department of the Spanish Government. The authors would like to thank Betsaide, S.A.L., Fytasa, S.A. and TS Fundiciones, S.A. Foundries for all the collaborating efforts made in order to elaborate the alloys and to obtain the samples.

REFERENCES

1. Lalich M. J., Loper C. R., "Effects of Pearlite Promoting Elements on the Kinetics of the Eutectoid Transformation in Ductile Cast Irons", AFS Transactions, vol. 81, pp 217-228 (1973).
2. Pan E. N., Lou M. S., Loper C. R., "Effects of Copper, Tin, and Manganese on the Eutectoid Transformation of Graphitic Cast Irons", AFS Transactions, vol. 95, pp 819-840, (1987).
3. Lacaze J., Boudot A., Gerval V., Oquab D., Santos H., "The Role of Manganese and Copper in the Eutectoid Transformation of Spheroidal Graphite Cast Iron", Metallurgical and Materials Transactions, vol. 28A, pp 2015-2025 (1997).
4. Lacaze J., Ford S., Wilson C., Dubu E., "Effects of Alloying Elements Upon the Eutectoid Transformation in As-Cast Spheroidal Graphite Cast Iron", Scandinavian Journal of Metallurgy, vol. 22, pp 300-309 (1993).
5. Lacaze J., Wilson C., Bak C., "Experimental Study of the Eutectoid Transformation in As-Cast Spheroidal Graphite Cast Iron", Scandinavian Journal of Metallurgy, vol. 23, pp 151-163 (1994).
6. Linares E., Gerval V., Lacaze J., "On the Characteristic Temperatures of the Eutectoid Reaction in Cast Irons", Scripta Materialia, vol. 38, pp 279-285 (1998).
7. Gerval V., Lacaze J., "Critical Temperature Range in Spheroidal Graphite Cast Iron", Iron and Steel Institute of Japan International, vol. 40, pp 386-302 (2000).
8. Lacaze J., "Pearlite Growth in Cast Irons: A Review of Literature Data", International Journal of Cast Metal Research, vol. 11, pp 431-436 (1999).
9. Larrañaga P., Gutiérrez J. M., Loizaga A., Sertucha J., Suárez R., "A Computer-Aided System for Melt Quality and Shrinkage Propensity Evaluation Based on the Solidification Process of Ductile Iron", AFS Transactions, vol. 116, pp 547-561 (2008).
10. Ågren, J., "Computer Simulations of the Austenite/Ferrite Diffusional Transformations in Low Alloyed Steels", Acta Materialia, vol. 30, pp 841-851 (1982).

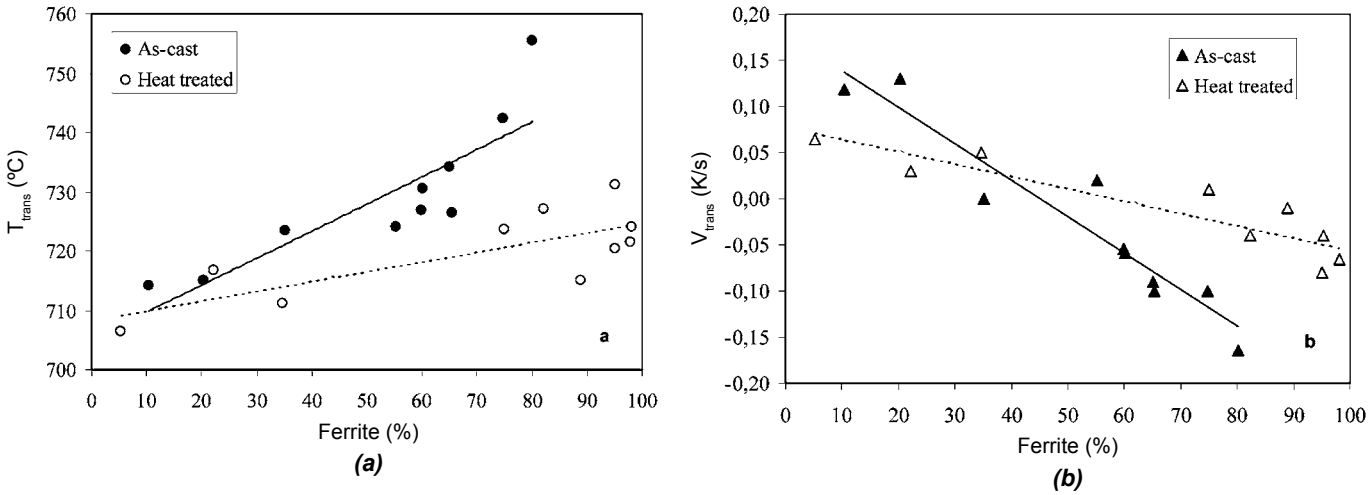

Figure 9. Evolution of the ferrite fraction versus T_{trans} (a) and V_{trans} (b) for as-cast and heat treated samples (V_{cool} = 34-60 K/min).